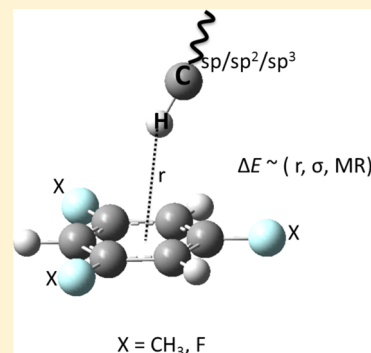


C–H $\cdots\pi$  Interactions and the Nature of the Donor Carbon AtomBrijesh Kumar Mishra,<sup>†</sup> Milind Madhusudan Deshmukh,<sup>‡</sup> and Ramanathan Venkatnarayan<sup>\*,§,#</sup><sup>†</sup>International Institute of Information Technology Bangalore, Bangalore 560100, Karnataka, India<sup>‡</sup>Department of Chemistry, Dr. Harisingh Gour Central University, Sagar 470003, Madhya Pradesh, India<sup>§</sup>School of Chemical and Biotechnology, SASTRA University, Thanjavur 613401, Tamil Nadu, India

## S Supporting Information

**ABSTRACT:** The influence of multiple substituents (F, CH<sub>3</sub>, NO<sub>2</sub>, CN, Cl, OH and NH<sub>2</sub>) on the C–H $\cdots\pi$  interaction in benzene–ethylene complex was investigated using the estimated CCSD(T) method and complete basis set limit. The results were compared with our earlier reported complexes of benzene–acetylene and benzene–methane, thus completing the sp, sp<sup>2</sup> and sp<sup>3</sup> series of C–H donors. The stabilization energy values for multiple fluoro-substituted benzene–ethylene complexes are found to be very close to those of the multiple fluoro-substituted benzene–methane complexes. Expectedly, the stabilization energies for the multiple methyl-substituted benzene–ethylene complexes lie between those of the multiple methyl-substituted benzene–methane and benzene–acetylene complexes. Energy decomposition analysis using the DFT-SAPT method predicts the dispersion energy to be dominant, similar to the benzene–methane complexes. For the symmetrically disubstituted complexes (–OH, –Cl, –NH<sub>2</sub>, –CN and –NO<sub>2</sub>), additional C–H $\cdots$ X interaction was observed, possibly due to the angular orientation of the ethylene molecule. Multidimensional correlation analysis between the electrostatic, dispersion and exchange–repulsion with the C–H $\cdots\pi$  interaction distance ( $r$ ), Hammett constant ( $\sigma$ ) and the molar refractivity (MR) revealed strong correlation between dispersion energy and the C–H $\cdots\pi$  interaction distance ( $r$ ) as well as molar refractivity (MR).



## ■ INTRODUCTION

Weak interactions, particularly the C–H $\cdots\pi$  interactions, have been an area of interest given their widespread role in chemistry and biology. A typical C–H $\cdots\pi$  complex consists of an aliphatic/aromatic C–H donor and a  $\pi$ -face of aromatic moieties as an acceptor. The role of such weak yet vital interactions in stabilizing crystal packings<sup>1–4</sup> and molecular clusters,<sup>5–7</sup> in influencing three-dimensional structure of biomolecules<sup>8–10</sup> and in the area of rational drug design is well recognized.<sup>11–13</sup> For example, Plevin et al. analyzed a database of 183 protein X-ray structures and nearly 3% of the methyl groups and 15% of the aromatic residues were found to be involved in C–H $\cdots\pi$  interactions.<sup>14</sup> The database search results were validated using the high-resolution NMR spectroscopy. Nishio and co-workers made a noteworthy contribution<sup>15,16</sup> and have made an exhaustive database pertaining to various roles of the C–H $\cdots\pi$  interactions.<sup>17</sup> Their crystal structure database study revealed that nearly 40% of the organic crystals possess C–H $\cdots\pi$  contacts.<sup>18</sup> Recently, Berg et al. reported the thermodynamic profiles for acetylcholinesterase (also known as AChE) and its two enantiomers, wherein the difference in enthalpy–entropy contribution was attributed to the C–H $\cdots\pi$  interactions between an activated C–H group and a  $\pi$ -face of the tyrosine residue.<sup>19</sup> The hydrogen bond nature of the C–H $\cdots\pi$  interaction in the haloethane–ethene was suggested by the atoms-in-molecules (AIM) study, and it was reported that the highly electronegative groups adjacent to the C–H bond

“activates” the C–H $\cdots\pi$  interactions.<sup>20</sup> Thus, generally, the C–H $\cdots\pi$  interactions are categorized as the weakest class of hydrogen bonds.<sup>21</sup>

Tsuzuki and co-workers made significant contribution by studying the C–H $\cdots\pi$  interactions in small model systems employing both theoretical and experimental techniques. The binding energy for the C–H $\cdots\pi$  interaction in the benzene–methane complexes was reported to be  $D_0 = 1.03$ – $1.13$  kcal/mol using mass-analyzed threshold ionization (MATI) spectroscopy.<sup>22</sup> Later, the C–H $\cdots\pi$  interaction for the benzene–ethylene and benzene–acetylene was measured to be  $1.4 \pm 0.2$  and  $2.7 \pm 0.2$  kcal/mol, respectively, by two-color multiphoton ionization spectroscopy.<sup>23</sup> Clearly, the interaction energy increases with the acidity of the C–H bonds involved in the C–H $\cdots\pi$  contacts. Fujii et al. measured the C–H $\cdots\pi$  interaction in benzene–ethane ( $D_0 = 1.6$  kcal/mol), benzene–propane ( $D_0 = 2.2$  kcal/mol), benzene–*n*-butane ( $D_0 = 2.7$  kcal/mol), benzene–isobutane ( $D_0 = 2.7$  kcal/mol) and benzene–cyclohexane ( $D_0 = 2.7$  kcal/mol) using two-color resonant two-photon ionization spectroscopy.<sup>24</sup> The  $D_0$  values computed at the CCSD(T) level were found to be in good agreement with the corresponding experimental values in gas phase, which clearly shows the strength of the CCSD(T) method.<sup>22–24</sup> Energy decomposition analysis revealed that the correlation energy (which was assumed to be mainly the

Received: June 5, 2014

Published: August 26, 2014



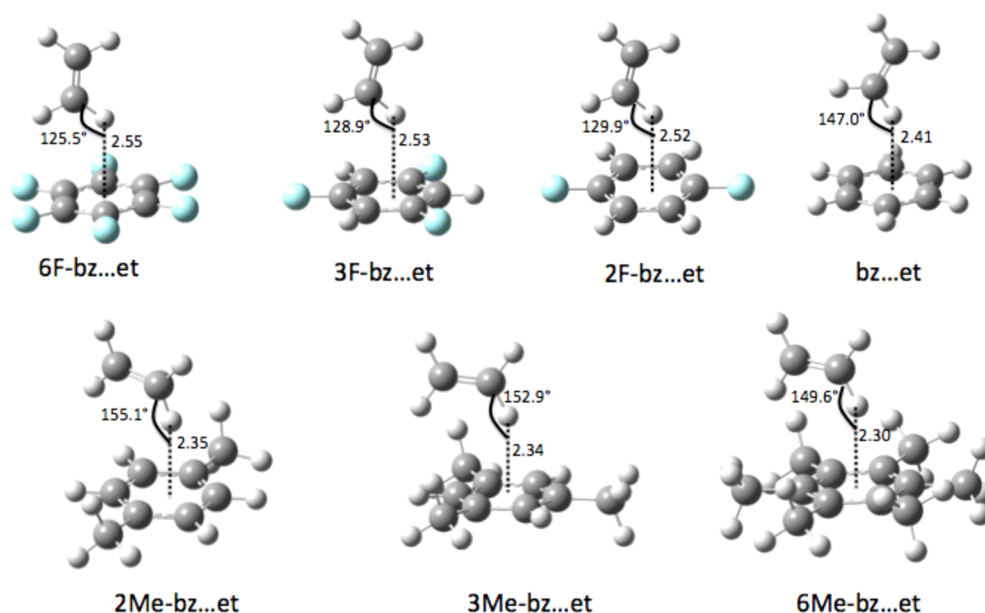


**Figure 1.** Optimized geometries of all 1:1 multiple fluoro- and methyl-substituted benzene with ethylene calculated at the MP2/aug-cc-pVDZ level of theory.

dispersion term) ranges from  $\sim 2.0$  to  $\sim 6.0$  kcal/mol, while the electrostatic energy term ranges from  $-0.2$  to  $-0.5$  kcal/mol, except for the case of benzene–acetylene, for which the electrostatic energy component was determined to be  $-1.7$  kcal/mol.<sup>25</sup> Therefore, it was understood that the correlation energy or the dispersion energy is the primary source of attraction in the C–H $\cdots\pi$  clusters.

The interaction strength between a C–H-donor and  $\pi$ -acceptor depends on the substituents present in their local environment. Recently, we showed that the C–H $\cdots\pi$  interaction energy in the benzene–acetylene complex could be tuned up to  $\sim 5.0$  kcal/mol by replacing the hydrogen atoms of benzene by multiple fluoro/methyl groups.<sup>26</sup> The trend in the interaction energy was rationalized successfully in terms of electron-donating (resonance) and electron-withdrawing (induction) effect of the substituent. Also, based on the results obtained using the DFT-SAPT/aug-cc-pVDZ, we showed that in some cases the electrostatic energy could be comparable to the dispersion energy, which is contrary to the general understanding that the dispersion energy is the dominant force in the C–H $\cdots\pi$  complexes.<sup>26</sup> However, the readers should keep in mind that the aug-cc-pVDZ basis set could underestimate the dispersion energy term as large as by  $\sim 15\%$ .<sup>27</sup> In the case of a benzene–methane complex, we showed that the multiple fluoro-substitution does not influence the interaction energy, while for multiple methyl-substitutions the interaction energy increases systematically with an increase in the methyl groups.<sup>28</sup> Recently, Bloom et al. extensively investigated the influence of various monosubstituents on the X–H $\cdots\pi$  clusters, where X = B, C, N, O, F.<sup>29</sup> In the case of X = F, NH<sub>2</sub>, OH, the electrostatic energy was found to be dominant contribution, while the dispersion energy was found to be more significant for the case of X = BH<sub>2</sub> and CH<sub>3</sub>.<sup>29</sup> The study for mono-, di- and trisubstituted halomethane with benzene revealed that the interaction energy increases with an increase in halogen atoms and the interaction energy for benzene $\cdots$ CHCl<sub>3</sub> is comparable to that of a conventional hydrogen bond.<sup>30</sup> Some other relevant studies include the interaction energy for benzene $\cdots$ methane, toluene $\cdots$ methane, *p*-xylene $\cdots$ methane, mesitylene $\cdots$ methane

and naphthalene $\cdots$ methane reported by Morita et al.,<sup>31</sup> the interaction energy for C<sub>6</sub>F<sub>6</sub> $\cdots$ methane cluster reported by Raju et al.,<sup>32</sup> the experimental study of the benzene–acetylene complex using Fourier-transform microwave spectroscopy by Ulrich et al.,<sup>33</sup> the computational study of the C–X $\cdots\pi$  type of interaction in substituted benzene $\cdots$ chloroacetylene complexes by Karthikeyan and Lee<sup>34</sup> and combined experimental–theoretical study of phenylacetylene dimer by Hobza and co-workers.<sup>35</sup>

Recently, we reported the influence of multiple substituents on the CH $\cdots\pi$  interaction in the benzene–acetylene (bz $\cdots$ ac) and benzene–methane (bz $\cdots$ me) complex.<sup>26,28</sup> The next logical candidate is benzene–ethane (bz $\cdots$ et) complex. While the carbon atom involved in the C–H $\cdots\pi$  interaction in the cases of benzene–acetylene and benzene–methane are of  $sp$  and  $sp^3$  nature, respectively, the ethane molecule has  $sp^2$  hybridized carbon atom. Thus, it serves as an intermediate between the two and thus gives a complete comparative analysis of the C–H $\cdots\pi$  interaction. Similarly to our previous works, fluorine and methyl groups were selected as primary substituents. The following aromatic moieties were chosen: symmetrically substituted difluorobenzene (2F-bz), symmetrically substituted trifluorobenzene (3F-bz) and hexafluorobenzene (6F-bz). Similarly the methyl-substituted complexes were also chosen. In addition to these, the influence of some other key substituents (NO<sub>2</sub>, CN, Cl, OH and NH<sub>2</sub>) was also studied. A comparison on the multiple substituents' effect on the C–H $\cdots\pi$  interaction in benzene–acetylene, benzene–ethylene and benzene–methane was examined.

## METHODOLOGY

The methodology adopted in this work follows the one used by us in our earlier studies involving acetylene and methane complexes.<sup>26,28</sup> Briefly, the MP2/aug-cc-pVDZ, MP2/aug-cc-pVTZ and CCSD(T)/aug-cc-pVDZ computations were performed using Gaussian 09 suite of programs.<sup>36</sup> The geometries of all the complexes were optimized using the MP2/aug-cc-pVDZ level of theory. The single-point MP2/aug-cc-pVTZ and CCSD(T)/aug-cc-pVDZ energy calculations were performed with frozen geometries obtained at the MP2/aug-cc-

pVDZ level. The core electrons were kept frozen in all the calculations. All energies were corrected for the basis set superposition error (BSSE), using the counterpoise-correction (CP) method.<sup>37</sup> The MP2/CBS energy values were determined by extrapolating the MP2/aug-cc-pVDZ and MP2/aug-cc-pVTZ energy values, with the two-point extrapolation scheme proposed by Helgaker et al.,<sup>38</sup> the estimated CCSD(T)/CBS energy was calculated using the following formula:

$$\text{est. } \Delta E_{\text{CCSD(T)/CBS}} = \Delta E_{\text{MP2/CBS}} + (\Delta E_{\text{CCSD(T)/aug-cc-pVDZ}} - \Delta E_{\text{MP2/aug-cc-pVDZ}})$$

For the energy decomposition, the DFT-SAPT method has been used frequently due to the trade-off between accuracy and computational power required.<sup>39–42</sup> The DFT-SAPT(PBE0)/aug-cc-pVDZ calculations for each of the complexes were carried out using the MOLPRO suite.<sup>43</sup> The  $E_{\text{exch-ind}}$  and  $E_{\text{exch-disp}}$  interaction terms were summed in the energy terms  $E_{\text{ind}}$  and  $E_{\text{disp}}$  respectively. For a few complexes, an efficient density fitting approximation to DFT-SAPT (DF-DFT-SAPT) in conjunction with aug-cc-pVDZ and aug-cc-pVTZ basis set was also employed. These calculations enable us to estimate the error associated due to size of the basis set. It was reported that with suitable auxiliary basis set the errors due to the approximation is insignificant; a detailed description regarding the DF-DFT-SAPT method can be found in ref 44.

## RESULTS AND DISCUSSION

**Geometries of Substituted Benzene...Ethylene Complexes.** The optimized geometries of all the 1:1 multiple fluoro- and methyl-substituted benzene with ethylene complexes were calculated at the MP2/aug-cc-pVDZ level of theory and are depicted in Figure 1. We have carried out vibrational frequency calculations at the same level of theory and basis set. We found that most of the geometries indeed represent true minimum energy geometry. Some of the geometries have small imaginary frequency (less than  $50 \text{ cm}^{-1}$ ); therefore, these geometries could be safely considered as near-equilibrium geometries. The details of the frequency calculations are summarized in Table S1 (Supporting Information, SI). The effect of different substituents is reflected on the corresponding C–H... $\pi$  distances and angles. For instance, upon going from the fluoro-substituted benzene to methyl-substituted benzene through the unsubstituted benzene, the C–H... $\pi$  distance gradually decreases. On the other hand, the corresponding C–H... $\pi$  angle increases when going from fluoro substitution to methyl substitution on benzene. It should be noted that the C–H... $\pi$  angles suggest directionality of the interaction. Within the given substitution type (fluoro or methyl), the geometrical changes are small but significantly different from that of unsubstituted benzene...ethylene complex. These geometrical parameters indicate that the C–H... $\pi$  interactions in methyl-substituted complexes would be much stronger than those in the fluoro-substituted ones. The trend observed in the C–H... $\pi$  distances in all the complexes involving the substituted benzenes with ethylene is not very different from the trends seen earlier in the case of complexes with acetylene and methane as listed in Table S1A (SI). It should be noted (in Table S1A (SI)) that while moving from acetylene ( $\text{sp}$  hybridized) to ethylene ( $\text{sp}^2$  hybridized) to methane ( $\text{sp}^3$  hybridized) complexes, the C–H... $\pi$  distance increases; this increase is consistent in all the substituted and unsubstituted complexes, leading to the expectation that the strength of the C–H... $\pi$  interaction decreases when we move from  $\text{sp}$  to  $\text{sp}^2$  to  $\text{sp}^3$  carbon atom. In Table S1B (SI) we list the interaction energies calculated at the MP2/aug-cc-pVDZ, MP2-cc-pVTZ and CCSD(T)/aug-cc-pVDZ levels, for the purpose of judging

the accuracy of the estimation of the basis set and understanding the effects of electron correlation beyond the MP2 method. It is to be noted that our interaction energy for the benzene–ethylene complex ( $-1.75 \text{ kcal/mol}$ ) is different than the one reported by Shibasaki et al.<sup>22</sup> ( $-2.17 \text{ kcal/mol}$ ) at the est. CCSD(T)/CBS. The difference may arise mainly because the geometry used in ref 22 was optimized using the cc-pVTZ basis set, which gave  $r = 2.52 \text{ \AA}$ , while we have used the aug-cc-pVDZ basis set, which yielded  $r = 2.41 \text{ \AA}$ .

**C–H... $\pi$  Interaction Energy in the Substituted Benzene...Ethylene Complexes.** In our earlier work, we have reported C–H... $\pi$  interaction energies in similarly substituted benzenes by taking acetylene and methane as C–H donors. These two C–H donors contain  $\text{sp}$  and  $\text{sp}^3$  hybridized carbon atoms, respectively. In this study we have considered ethylene to cover the third possibility, where the donor has  $\text{sp}^2$  hybridized carbon atom. In Figure 2 we have

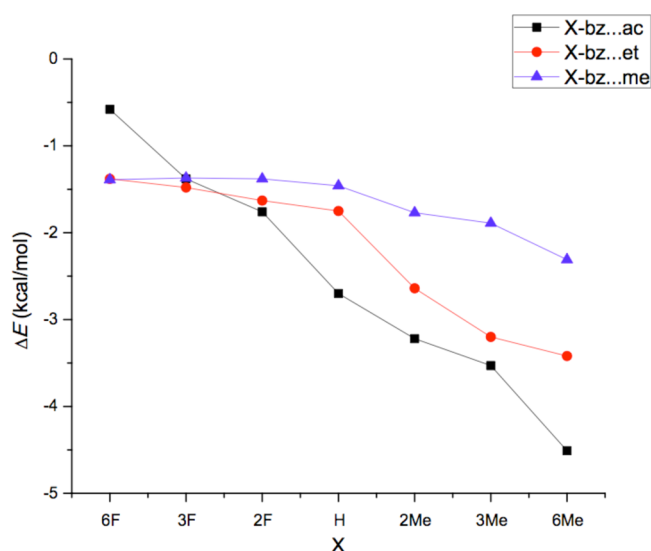


**Figure 2.** Interaction energy (at the est. CCSD(T)/CBS) in kcal/mol for multiple fluoro- and methylsubstituted benzene with acetylene,<sup>26</sup> ethylene and methane.<sup>28</sup>

depicted the interaction energy of all the complexes of fluoro- and methyl-substituted benzenes with acetylene, ethylene and methane. The interaction energy for the benzene–ethylene complex was computed to be  $-1.75 \text{ kcal/mol}$  at the est. CCSD(T)/CBS method. It is to be noted that Tsuzuki et al. reported the experimental interaction energy ( $D_0$ ) for the benzene–ethylene complex to be  $1.4 \pm 0.2 \text{ kcal/mol}$ .<sup>22</sup> For comparing computed interaction energies with the experimental interaction energies, one has to account for correction due to vibrational zero-point energy (ZPE). The change in zero-point energy ( $\Delta\text{ZPE}$ ) upon complex formation was determined to be in the range of  $0.60\text{--}0.90 \text{ kcal/mol}$  for substituted benzenes...ethylene complexes (Table S1C (SI)). The interaction energies (predicted using est. CCSD(T)/CBS method; Table S1A (SI)) corresponding to the ethylene complexes lie approximately between the interaction energies of acetylene and methane complexes. Clearly, the electron withdrawing group (fluoro-substituents) weakens the benzene–ethylene complex while the electron donating group (methyl) strengthens the complex. Interestingly, from both Figure 2 and Table S1A (SI), we see that the interaction energy for the fluoro-substituted complex does not change as

appreciably as the interaction energy for the methyl-substituted complexes. For example, the interaction energy for hexamethyl-substituted benzene–ethylene complex becomes nearly double of that of the benzene–ethylene complex, while hexafluorobenzene...ethylene is only slightly less stable ( $\sim 0.4$  kcal/mol) than the benzene...ethylene complex. Unlike the group of complexes with acetylene and methane, where we could estimate the increase in the interaction energy per methyl substituent as approximately  $-0.3$  and  $-1.5$  kcal/mol, respectively, we are unable to estimate similar interaction energy per methyl substituent in the case of ethylene complexes. We suspect steric hindrance to be the major cause for such a trend in the ethylene complexes.

#### C–H... $\pi$ Interaction Energy Decomposition: DFT-SAPT

**Results.** Decomposing the interaction energy into its various contributing constituents, namely electrostatic ( $E_{\text{elec}}$ ), dispersion ( $E_{\text{disp}}$ ), exchange-repulsion ( $E_{\text{exch}}$ ) and induction ( $E_{\text{ind}}$ ), helps to better characterize the C–H... $\pi$  interaction. The result of this decomposition analysis is shown in Figure 3. In our

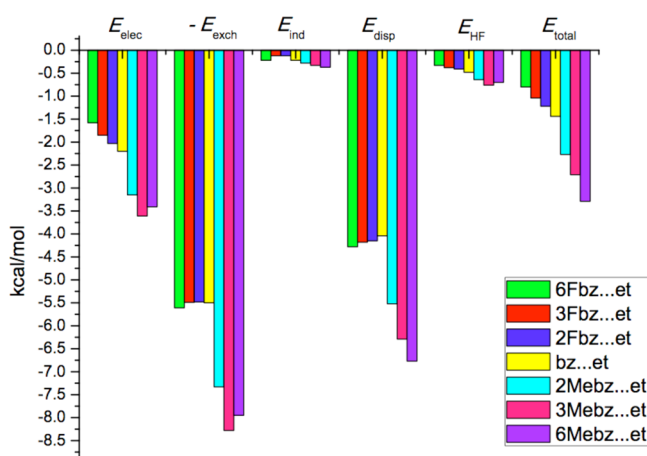


**Figure 3.** Energy decomposition results obtained using the DFT-SAPT method for multiple fluoro- and methyl-substituted benzene...ethylene complexes.

earlier work we had reported similar energy decomposition values for the groups of complexes with acetylene and methane and they are shown in Table 1 along with the energy decomposition values for the complexes with ethylene.

As seen from Table 1, the dispersion energy ( $E_{\text{disp}}$ ) is the major contributor to the stabilization for the ethylene complexes and is highest when these values are compared across the complexes of acetylene and methane. The next major contributor to the stabilization is the electrostatic component

( $E_{\text{elec}}$ ). The  $E_{\text{elec}}$  values are highest for the ethylene complexes vis-a-vis methane and acetylene complexes for fluoro-substituted complexes. However, for methyl-substituted complexes the  $E_{\text{elec}}$  values for ethylene complexes fall between those of methane and acetylene complexes. The other components, namely the induction ( $E_{\text{ind}}$ ) and higher order contribution ( $d_{\text{HF}}$ ) values are relatively small and they lie between those of acetylene and methane complexes. In order to compare and visualize the relative proportion of the  $E_{\text{elec}}$  and  $E_{\text{disp}}$ , we plotted the ratio  $E_{\text{disp}}/E_{\text{elec}}$  for various substitutions for all the three groups of complexes, as depicted Figure 4. It is apparent from

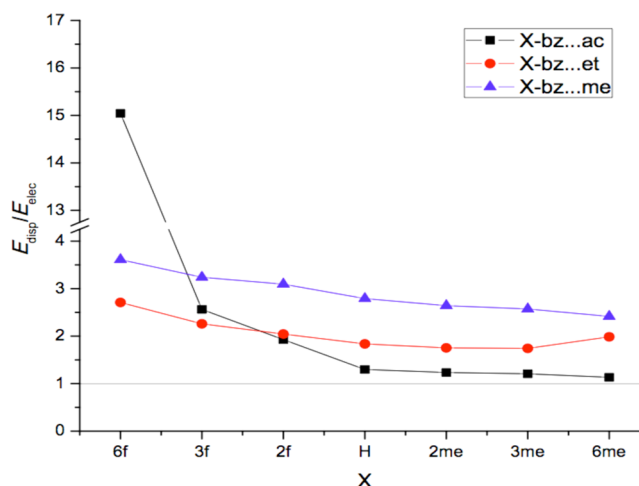


**Figure 4.** Relative proportion of  $E_{\text{elec}}$  and  $E_{\text{disp}}$ . Two dominant components in the interaction energy.

Figure 4 that the  $E_{\text{disp}}$  component is 2 to 3 times larger than the  $E_{\text{elec}}$  component in the case of substituted benzene–ethylene complex, and 3 to 4 times more dominant in the case of methane complexes. In the case of substituted benzene–acetylene complex, we observe a dramatic trend, where  $E_{\text{disp}}$  is 2 to 15 times more dominant than  $E_{\text{elec}}$  for the fluoro substitution, whereas both  $E_{\text{disp}}$  and  $E_{\text{elec}}$  components are almost equally dominant for the methyl substitutions.

It is generally observed that the aug-cc-pVDZ basis set underestimates the dispersion interaction energy term. We have attempted to quantify this underestimation by performing density-fitting approximation to the DFT-SAPT calculations using the aug-cc-pVTZ basis set for 4 complexes. The results are listed in Supporting Information (Table S2). Here we wish to emphasize that the error due to density-fitting approximation is found to be negligible. We found that the dispersion energy term is underestimated by nearly 10% at the aug-cc-pVDZ basis

**Table 1.** Energy Decomposition Results Obtained Using the DFT-SAPT Method for Multiple Fluoro- and Methyl- Substituted Benzene...Ethylene Complexes

	$-E_{\text{elec}}$			$-E_{\text{ind}}$			$-E_{\text{disp}}$			$E_{\text{exch}}$			$-d_{\text{HF}}$			$-E_{\text{tot}}$		
	sp	sp <sup>2</sup>	sp <sup>3</sup>	sp	sp <sup>2</sup>	sp <sup>3</sup>	sp	sp <sup>2</sup>	sp <sup>3</sup>	sp	sp <sup>2</sup>	sp <sup>3</sup>	sp	sp <sup>2</sup>	sp <sup>3</sup>	sp	sp <sup>2</sup>	sp <sup>3</sup>
6F	0.23	1.58	0.64	0.52	0.22	0.10	3.46	4.28	2.31	4.53	5.61	2.02	0.36	0.33	0.09	0.03	0.80	1.13
3F	1.44	1.85	0.71	0.47	0.12	0.05	3.69	4.18	2.30	5.23	5.49	2.03	0.53	0.38	0.12	0.91	1.04	1.15
2F	1.92	2.03	0.75	0.48	0.12	0.05	3.70	4.15	2.32	5.28	5.48	2.08	0.94	0.41	0.13	1.76	1.22	1.17
6H	2.89	2.20	0.86	0.55	0.22	0.10	3.75	4.04	2.40	5.46	5.50	2.23	0.72	0.48	0.16	2.54	1.44	1.27
2Me	3.59	3.15	1.09	0.66	0.28	0.12	4.43	5.52	2.88	6.57	7.33	2.71	0.91	0.64	0.20	3.01	2.27	1.58
3Me	3.97	3.61	1.19	0.72	0.33	0.14	4.79	6.29	3.06	7.18	8.28	2.89	1.01	0.76	0.22	3.32	2.71	1.71
6Me	5.08	3.41	1.56	0.90	0.37	0.18	5.75	6.77	3.67	9.04	7.95	3.56	1.34	0.70	0.29	4.04	3.29	2.10



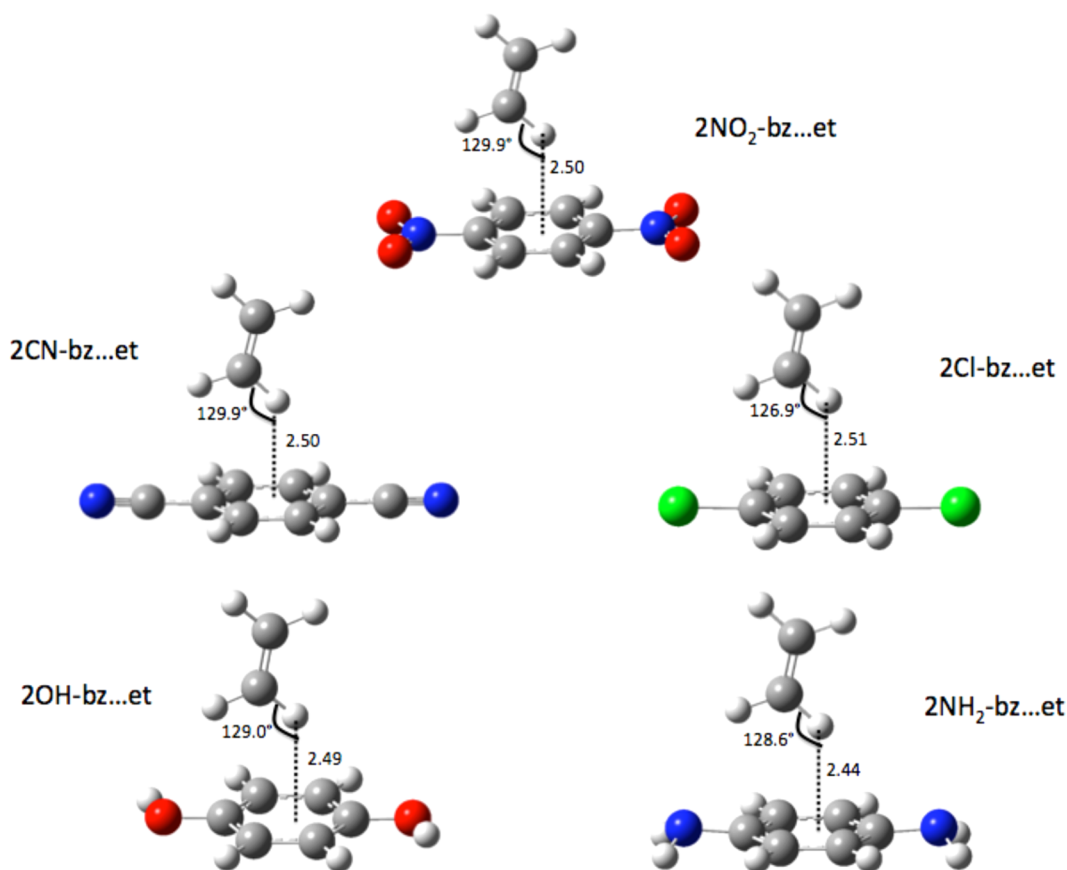


Figure 5. Optimized geometries of all 1:1 symmetrical disubstituted benzenes with ethylene calculated at the MP2/aug-cc-pVDZ level of theory.

Table 2. Interaction Energies (in kcal/mol) and C–H... $\pi$  Distance in Å within Parentheses Obtained Using the est. CCSD(T)/CBS Method for Various Disubstituted Benzene...Acetylene, Ethylene and Methane Complexes

X	X-benzene...acetylene		X-benzene...ethylene		X-benzene...methane	
	$C^{sp}-H\cdots\pi^a$		$C^{sp^2}-H\cdots\pi$		$C^{sp^3}-H\cdots\pi^b$	
2NO <sub>2</sub>	−0.99	(2.474)	−1.47	(2.500)	−1.48	(2.654)
2CN	−1.15	(2.472)	−1.59	(2.500)	−1.45	(2.652)
2Cl	−1.98	(2.422)	−2.60	(2.510)	−1.55	(2.637)
2OH	−2.77	(2.375)	−2.66	(2.490)	−1.56	(2.654)
2NH <sub>2</sub>	−3.08	(2.366)	−3.18	(2.440)	−1.79	(2.609)

<sup>a</sup>ref 26. <sup>b</sup>ref 28.

2Cl-bz...et	2Cl-bz...et(rot)	2OH-bz...et	2OH-bz...et(rot)
$\Delta E = -2.60$ kcal/mol	$\Delta E = -0.97$ kcal/mol	$\Delta E = -2.66$ kcal/mol	$\Delta E = -1.44$ kcal/mol

Figure 6. Geometry of 2Cl-bz...et, 2Cl-bz...et(rot), 2OH-bz...et and 2OH-bz...et(rot) and their interaction energies at est. CCSD(T)/CBS method.

set, when compared to that at the aug-cc-pVTZ basis set. Thus, for the purpose of quantitative analysis the reader should be aware of this caveat.

We have also studied the ethylene complex with various other (di)substituents like NO<sub>2</sub>, Cl, NH<sub>2</sub>, CN and OH that are representatives of both electron-withdrawing and -donating natures. The optimized geometry for these disubstituted benzenes with ethylene is shown in Figure 5 wherein we see

that the interaction distance remains almost unchanged for the NO<sub>2</sub>, Cl, CN, and OH substituents ( $\sim 2.5$  Å) and is slightly reduced to 2.44 Å in the case of NH<sub>2</sub> substituent. The interaction energies for all these disubstituted benzenes are summarized in Table 2 wherein the interaction energies for the acetylene and methane complexes are also listed in order to get a comparative understanding for the three types of carbons. Interestingly, we observed that the interaction energies for the

ethylene complexes do not lie in between those of the acetylene and methane. Although the acidic nature of the hydrogen atom in ethylene is lesser than that of the hydrogen atom in acetylene, we see that ethylene has the most stable complexes with CN, Cl, OH and  $\text{NH}_2$ . It appears that due to the angular orientation of the ethylene molecule there is a possibility of another  $\text{C}-\text{H}\cdots\text{X}$  ( $\text{X} = \text{N}, \text{Cl}, \text{O}$ ) interaction in addition to the  $\text{C}-\text{H}\cdots\pi$  interaction, which could be attributed to the enhanced stability. To verify this, the ethylene molecule was rotated by  $90^\circ$  while keeping the  $\text{C}-\text{H}\cdots\pi$  distance fixed as depicted in Figure 6. The interaction energies for the two newly constructed geometries  $2\text{Cl-bz}\cdots\text{et}(\text{rot})$  and  $2\text{OH-bz}\cdots\text{et}(\text{rot})$  were computed to be  $-0.97$  kcal/mol and  $-1.44$  kcal/mol, respectively, which is significantly lower than their counterparts. We have also carried out similar computations for the benzene–ethylene complex by rotating the ethylene molecule over the benzene moiety. The results are listed in Supporting Information, Table S3. From the results, it is clear that in the unsubstituted benzene–ethylene complex, the interaction energy is almost invariant to the orientation of the ethylene molecule. These additional data clearly indicate the presence of weak stabilizing interaction of type  $\text{C}-\text{H}\cdots\text{X}$  between the two moieties. Therefore, it can be safely deduced that the orientation of ethylene plays a significant role in stabilizing substituted benzene–ethylene complexes.

**Multidimensional Correlation Analysis.** The effect of various substituents on the reactivity of aromatic moieties has been of considerable interest for having the molecular level insights about formation of weak complexes. Suresh et al. made one such early attempt by using molecular electrostatic potential (MESP) topography.<sup>45–48</sup> It was reported that the substituent effects are nicely reflected in terms of MESP values at the (3, +3) minimum ( $V_{\min}$ ) over the aromatic ring. Further the position of the MESP (3, +3) minimum determines the interaction site. Recently, they used the  $V_{\min}$  values to gauge the strength of the cation– $\pi$  interactions.<sup>49–51</sup> In the present work, we too analyzed the effect of various multiple substituents on the reactivity of the aromatic ring in terms of  $V_{\min}$  and the corresponding Hammett constant ( $\sigma$ ). For the calculation of the MESP topography, a program developed by Gadre and co-workers was used; for details, see refs S2 and S3. We also found a good correlation between  $\sigma$  and  $V_{\min}$  over the aromatic ring, as depicted in Figure 7. This suggests that  $V_{\min}$  indeed reflects the substituent's effect on the reactivity of the aromatic ring. For instance, electron-donating substituents, such as methyl and  $\text{NH}_2$ , would activate the aromatic ring, which is reflected in a more negative  $V_{\min}$  value for these cases (see Supporting Information Table S4). To the contrary, electron-withdrawing substituents deactivate the aromatic ring, and the  $V_{\min}$  value

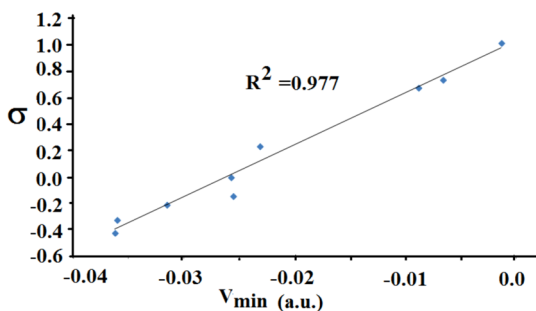


Figure 7. Correlation between  $\sigma$  and  $V_{\min}$ .

becomes less negative with respect to that of the benzene (cf. Table S4 (SI)). Furthermore, very strong electron withdrawing substituents completely deactivate the aromatic ring, which is evident from the absence of (3, +3) MESP minimum over the aromatic ring in these cases.

Recently, Wheeler and co-workers carried out multidimensional correlation analysis between the different components of energy with Hammett constant ( $\sigma$ ), molar refractivity (MR), the  $\text{C}-\text{H}\cdots\pi$  interaction distance ( $r$ ) and various combinations of these parameters.<sup>29</sup> These authors reported that the electrostatic component strongly correlates with  $\sigma$  and  $r$ , the dispersion component correlates with a combination of  $r$  and MR and the exchange repulsion term correlates well only with  $r$ . Similarly, Deshmukh et al. found a linear correlation between the  $z$ -component of polarizability and the dispersion energy for the complexes of small molecules with the pyrazine dimer system.<sup>54</sup> We have also carried out similar multidimensional correlation analysis for the methane complexes in our earlier work.<sup>25</sup> In the present work, we also carried out a similar correlation analysis for substituted benzenes with ethylene/acetylene complexes and the results are summarized in Table 3.

**Table 3. Correlation Coefficients for the Exchange-Repulsion, Dispersion and Electrostatic Components for Various Disubstituted Benzene–Methane Complexes with Hammett Constants ( $\sigma$ ), Molar Refractivity (MR), Interaction Distance ( $r$ ) and Combination of These Constants**

	X-bz $\cdots$ ac						
	$\sigma$	$r$	MR	( $\sigma, r$ )	( $\sigma, \text{MR}$ )	( $r, \text{MR}$ )	( $\sigma, r, \text{MR}$ )
$E_{\text{elec}}$	0.91	0.81	0.75	1.00	1.00	0.84	1.00
$E_{\text{disp}}$	0.56	0.98	0.99	0.98	1.00	0.99	1.00
$E_{\text{exch}}$	0.62	0.96	0.97	0.97	1.00	0.97	1.00
	X-bz $\cdots$ et						
	$\sigma$	$r$	MR	( $\sigma, r$ )	( $\sigma, \text{MR}$ )	( $r, \text{MR}$ )	( $\sigma, r, \text{MR}$ )
$E_{\text{elec}}$	0.73	0.82	0.73	0.90	0.90	0.87	0.93
$E_{\text{disp}}$	0.45	0.95	0.92	0.95	0.95	0.92	0.96
$E_{\text{exch}}$	0.48	0.85	0.78	0.85	0.89	0.79	0.90
	X-bz $\cdots$ me						
	$\sigma$	$r$	MR	( $\sigma, r$ )	( $\sigma, \text{MR}$ )	( $r, \text{MR}$ )	( $\sigma, r, \text{MR}$ )
$E_{\text{elec}}$	0.67	0.98	0.95	1.00	1.00	0.98	1.00
$E_{\text{disp}}$	0.52	1.00	0.99	1.00	1.00	1.00	1.00
$E_{\text{exch}}$	0.57	1.00	0.98	1.00	0.99	1.00	1.00

In the case of complexes with ethylene, the MR, a measure of polarizability and  $r$  are seen to correlate well with the  $E_{\text{disp}}$  component. Contrary, the parameter  $\sigma$ , which is assumed to capture well the substituent's electrostatic property, does not correlate with  $E_{\text{elec}}$ , whereas the correlation with  $E_{\text{elec}}$  improves when  $\sigma$  and  $r$  are considered together. On the other hand, in the case of complexes with acetylene, the  $E_{\text{elec}}$  correlates well with  $\sigma$ , and this correlation improves further when  $\sigma$  is combined with  $r$  and/or MR. The dispersion component correlates excellently with  $r$  and MR. Interestingly, the correlation between  $E_{\text{elec}}$  and  $\sigma$  depends on the nature of the carbon atom involved, with largest value for the most acidic acetylene carbon atom and lowest in the case of the methane. Both the  $E_{\text{disp}}$  and  $E_{\text{exch}}$  components correlate consistently well with  $r$  for all the types of carbon atoms involved in the complexes.

## CONCLUDING REMARKS

In this work we have successfully compared the C–H $\cdots\pi$  interaction in substituted benzene with methane/ethylene/acetylene complexes, which span all the hybridization  $sp^3$ ,  $sp^2$ ,  $sp$  in the donor carbon atom. The motivation for this work has been to complete our investigation of the C–H $\cdots\pi$  interaction for all the different hybridizations of the donor carbon atom. Our analysis is based on the highly accurate energies obtained at the est. CCSD(T)/CBS level of theory. For fluoro-substitution the trend in the interaction energy for ethylene and methane complexes is very similar, while in the case of methyl substitution, the interaction energy lies between those of the methane and acetylene complexes. Upon the decomposition of the total interaction energy into various components, we see that the dispersion component is the most dominating and it is 2 to 3 times larger than the second dominating component (the electrostatic component). Multi-dimensional correlation analysis reveals that the  $E_{\text{elec}}$  component does not correlate with any of the three parameters for ethylene complexes, while  $E_{\text{disp}}$  correlates with  $r$  and MR significantly. In the case of other key substituents, we established that there exists an additional C–H $\cdots$ X type of interaction, which enhances the stability of the ethylene complexes compared to acetylene and methane complexes. This study would be particularly relevant in the area of rational drug design where by introducing various substituents in aromatic side-chains in proteins one would want to tune the binding affinity between aromatic side-chain and a small ligand.

## ASSOCIATED CONTENT

### Supporting Information

Table S1: Frequency analysis of all the complexes at MP2/aug-cc-pVDZ. Table S1A: Interaction energy (at the est. CCSD(T)/CBS) in kcal/mol and C–H $\cdots\pi$  distance in Å within parentheses for multiple fluoro- and methyl-substituted benzene with acetylene, ethylene and methane. Table S1B: Counterpoise-corrected interaction energy values (kcal/mol) at MP2/aug-cc-pVDZ, MP2/aug-cc-pVTZ and CCSD(T)/aug-cc-pVDZ level. Table S1C:  $\Delta$ ZPE values computed at MP2/aug-cc-pVDZ. Table S2: DFT-SAPT using aug-cc-pVTZ for the 4 complex. Table S3: Counterpoise-corrected interaction energies (kcal/mol) for benzene ethylene complex. Table S4: Electrostatic potential minimum ( $V_{\text{min}}$ ) over the aromatic ring in a.u., Hammett constant ( $\sigma$ ) and the binding energy with ethylene calculated at MP2/aug-cc-pVDZ and CCSD(T)/aug-cc-pVDZ level of theory in kcal mol $^{-1}$ . This material is available free of charge via the Internet at <http://pubs.acs.org>.

## AUTHOR INFORMATION

### Corresponding Author

\*E-mail: [vraman@scbt.sastra.edu](mailto:vraman@scbt.sastra.edu).

### Present Address

<sup>#</sup>(R.V.) Currently a visiting fellow at the Jawaharlal Nehru Centre for Advanced Scientific Research, Jakkur, Bangalore 560064, India.

### Notes

The authors declare no competing financial interest.

## ACKNOWLEDGMENTS

V.R. thanks SASTRA University for the computational infrastructure and funds for procuring Gaussian 09 suite of program.

## REFERENCES

- (1) Kobayashi, Y.; Saigo, K. *J. Am. Chem. Soc.* **2005**, *127*, 15054.
- (2) Umezawa, Y.; Tsuboyama, S.; Takahashi, H.; Uzawa, J.; Nishio, M. *Tetrahedron* **1999**, *55*, 10047.
- (3) Boese, R.; Clark, T.; Gavezzotti, A. *Helv. Chim. Acta* **2003**, *86*, 1085.
- (4) Nishio, M. *Phys. Chem. Chem. Phys.* **2011**, *13*, 13873.
- (5) Rahalkar, A.; Mishra, B.; Ramanathan, V.; Gadre, S. *Theor. Chem. Acc.* **2011**, *130*, 491.
- (6) Karthikeyan, S.; Lee, H. M.; Kim, K. S. *J. Chem. Theory Comput.* **2010**, *6*, 3190.
- (7) Majumder, M.; Mishra, B. K.; Sathyamurthy, N. *Chem. Phys. Lett.* **2013**, *557*, 59.
- (8) Tatko, C. D.; Waters, M. L. *J. Am. Chem. Soc.* **2004**, *126*, 2028.
- (9) Muktha, B.; Srinivas, O.; Amresh, M. R.; Guru Row, T. N.; Jayaraman, N.; Sekar, K. *Carbohydr. Res.* **2003**, *338*, 2005.
- (10) Riley, K. E.; Pitoňák, M.; Černý, J. i.; Hobza, P. *J. Chem. Theory Comput.* **2009**, *6*, 66.
- (11) Meyer, E. A.; Castellano, R. K.; Diederich, F. *Angew. Chem., Int. Ed. Engl.* **2003**, *42*, 1210.
- (12) Raju, R. K.; Burton, N. A.; Hillier, I. H. *Phys. Chem. Chem. Phys.* **2010**, *12*, 7117.
- (13) Ozawa, T.; Okazaki, K.; Kitauro, K. *J. Comput. Chem.* **2011**, *32*, 2774.
- (14) Plevin, M. J.; Bryce, D. L.; Boisbouvier, J. *Nat. Chem.* **2010**, *2*, 466.
- (15) Nishio, M.; Hirota, M.; Umezawa, Y. *The CH/ $\pi$  Interaction*; Wiley-VCH: New York, 1998.
- (16) Nishio, M.; Umezawa, Y.; Fantini, J.; Weiss, M. S.; Chakrabarti, P. *Phys. Chem. Chem. Phys.* **2014**, *16*, 12648.
- (17) The CH/ $\pi$  Institute. Database: List of papers relating to the CH/ $\pi$  hydrogen bond; <http://www.tim.hi-ho.ne.jp/dionisio/database.html> (accessed January 31, 2014).
- (18) Umezawa, Y.; Tsuboyama, S.; Honda, K.; Uzawa, J.; Nishio, M. *Bull. Chem. Soc. Jpn.* **1998**, *71*, 1207.
- (19) Berg, L.; Niemiec, M. S.; Qian, W.; Andersson, C. D.; Wittung-Stafshede, P.; Ekström, F.; Linusson, A. *Angew. Chem., Int. Ed.* **2012**, *51*, 12716.
- (20) Dom, J. J. J.; Michielsen, B.; Maes, B. U. W.; Herrebout, W. A.; van der Veken, B. J. *Chem. Phys. Lett.* **2009**, *469*, 85.
- (21) Ran, J.; Wong, M. W. *J. Phys. Chem. A* **2006**, *110*, 9702.
- (22) Shibasaki, K.; Fujii, A.; Mikami, N.; Tsuzuki, S. *J. Phys. Chem. A* **2006**, *110*, 4397.
- (23) Shibasaki, K.; Fujii, A.; Mikami, N.; Tsuzuki, S. *J. Phys. Chem. A* **2007**, *111*, 753.
- (24) Fujii, A.; Hayashi, H.; Park, J. W.; Kazama, T.; Mikami, N.; Tsuzuki, S. *Phys. Chem. Chem. Phys.* **2011**, *13*, 14131.
- (25) Tsuzuki, S. *Annu. Rep. Prog. Chem., Sect. C: Phys. Chem.* **2012**, *108*, 69.
- (26) Mishra, B. K.; Karthikeyan, S.; Ramanathan, V. *J. Chem. Theory Comput.* **2012**, *8*, 1935.
- (27) Rezáč, J.; Hobza, P. *J. Chem. Theory Comput.* **2011**, *7*, 685.
- (28) Karthikeyan, S.; Ramanathan, V.; Mishra, B. K. *J. Phys. Chem. A* **2013**, *117*, 6687.
- (29) Bloom, J. W. G.; Raju, R. K.; Wheeler, S. E. *J. Chem. Theory Comput.* **2012**, *8*, 3167.
- (30) Tsuzuki, S.; Honda, K.; Uchimaru, T.; Mikami, M.; Fujii, A. *J. Phys. Chem. A* **2006**, *110*, 10163.
- (31) Morita, S.-i.; Fujii, A.; Mikami, N.; Tsuzuki, S. *J. Phys. Chem. A* **2006**, *110*, 10583.
- (32) Raju, R. K.; Hillier, I. H.; Burton, N. A.; Vincent, M. A.; Doudou, S.; Bryce, R. A. *Phys. Chem. Chem. Phys.* **2010**, *12*, 7959.
- (33) Ulrich, N. W.; Seifert, N. A.; Dorris, R. E.; Peebles, R. A.; Pate, B. H.; Peebles, S. A. *Phys. Chem. Chem. Phys.* **2014**, *16*, 8886.
- (34) Karthikeyan, S.; Lee, J. Y. *Chem. Phys. Lett.* **2014**, *602*, 16.
- (35) Maity, S.; Patwari, G. N.; Sedlak, R.; Hobza, P. *Phys. Chem. Chem. Phys.* **2011**, *13*, 16706.
- (36) Frisch, M. J.; Trucks, G. W.; Schlegel, H. B.; Scuseria, G. E.; Robb, M. A.; Cheeseman, J. R.; Scalmani, G.; Barone, V.; Mennucci,

B.; Petersson, G. A.; Nakatsuji, H.; Caricato, M.; Li, X.; Hratchian, H. P.; Izmaylov, A. F.; Bloino, J.; Zheng, G.; Sonnenberg, J. L.; Hada, M.; Ehara, M.; Toyota, K.; Fukuda, R.; Hasegawa, J.; Ishida, M.; Nakajima, T.; Honda, Y.; Kitao, O.; Nakai, H.; Vreven, T.; Montgomery, Jr., J. A.; Peralta, J. E.; Ogliaro, F.; Bearpark, M.; Heyd, J. J.; Brothers, E.; Kudin, K. N.; Staroverov, V. N.; Kobayashi, R.; Normand, J.; Raghavachari, K.; Rendell, A.; Burant, J. C.; Iyengar, S. S.; Tomasi, J.; Cossi, M.; Rega, N.; Millam, J. M.; Klene, M.; Knox, J. E.; Cross, J. B.; Bakken, V.; Adamo, C.; Jaramillo, J.; Gomperts, R.; Stratmann, R. E.; Yazyev, O.; Austin, A. J.; Cammi, R.; Pomelli, C.; Ochterski, J. W.; Martin, R. L.; Morokuma, K.; Zakrzewski, V. G.; Voth, G. A.; Salvador, P.; Dannenberg, J. J.; Dapprich, S.; Daniels, A. D.; Farkas, Ö.; Foresman, J. B.; Ortiz, J. V.; Cioslowski, J.; Fox, D. J. *Gaussian 09*; Gaussian, Inc.: Wallingford, CT, 2009.

(37) Boys, S. F.; Bernardi, F. *Mol. Phys.* **1970**, *19*, 553.

(38) Helgaker, T.; Klopper, W.; Koch, H.; Noga, J. *J. Chem. Phys.* **1997**, *106*, 9639.

(39) Karthikeyan, S.; Sedlak, R.; Hobza, P. *J. Phys. Chem. A* **2011**, *115*, 9422.

(40) Kim, K. S.; Karthikeyan, S.; Singh, N. J. *J. Chem. Theory Comput.* **2011**, *7*, 3471.

(41) Maity, S.; Patwari, G. N.; Karthikeyan, S.; Kim, K. S. *Phys. Chem. Chem. Phys.* **2010**, *12*, 6150.

(42) Tekin, A.; Jansen, G. *Phys. Chem. Chem. Phys.* **2007**, *9*, 1680.

(43) Werner, H.-J. K., P. J.; Lindh, R.; Manby, F. R.; Schütz, M.; Celani, P.; Korona, T.; Rauhut, G.; Amos, R. D.; Bernhardsson, A.; Berning, A.; Cooper, D. L.; Deegan, M. J. O.; Dobbyn, A. J.; Eckert, F.; Hampel, C.; Hetzer, G.; Lloyd, A. W.; McNicholas, S. J.; Meyer, W.; Mura, M. E.; Nicklass, A.; Palmieri, P.; Pitzer, R.; Schumann, U.; Stoll, H.; Stone, A. J.; Tarroni, R.; Thorsteinsson, T. *MOLPRO*, ver. 2006.1; University College Cardiff Consultants Limited: Cardiff, Wales, U.K., 2006.

(44) Heßelmann, A.; Jansen, G.; Schütz, M. *J. Chem. Phys.* **2005**, *122*, 014103.

(45) Gadre, S. R.; Suresh, C. H. *J. Org. Chem.* **1997**, *62*, 2625.

(46) Suresh, C. H.; Gadre, S. R. *J. Am. Chem. Soc.* **1998**, *120*, 7049.

(47) Suresh, C. H.; Gadre, S. R. *J. Phys. Chem. A* **2007**, *111*, 710.

(48) Suresh, C. H.; Alexander, P.; Vijayalakshmi, K. P.; Sajith, P. K.; Gadre, S. R. *Phys. Chem. Chem. Phys.* **2008**, *10*, 6492.

(49) Sayyed, F. B.; Suresh, C. H. *Tetrahedron Lett.* **2009**, *50*, 7351.

(50) Sayyed, F. B.; Suresh, C. H.; Gadre, S. R. *J. Phys. Chem. A* **2010**, *114*, 12330.

(51) Sayyed, F. B.; Suresh, C. H. *J. Phys. Chem. A* **2011**, *115*, 9300.

(52) Balanarayan, P.; Gadre, S. R. *J. Chem. Phys.* **2003**, *119*, 5037.

(53) Roy, D.; Balanarayan, P.; Gadre, S. R. *J. Chem. Phys.* **2009**, *121*, 815.

(54) Deshmukh, M.; Sakaki, S. *Theor. Chem. Acc.* **2011**, *130*, 475.